

## Article

# Anti-Disturbance Integrated Control Method and Energy Consumption Analysis of Central Heating Systems Based on Resistance–Capacitance Reactance

Lu Jin <sup>1</sup>, Ligu Shi <sup>2</sup>, Dezhi Li <sup>1</sup>, Kaicheng Liu <sup>1</sup>, Ming Zhong <sup>1</sup> and Jingshuai Pang <sup>1,\*</sup>

<sup>1</sup> China Electric Power Research Institute Limited, Beijing 100192, China; jinlu@epri.sgcc.com.cn (L.J.); lidezhi@epri.sgcc.com.cn (D.L.); liukaicheng@epri.sgcc.com.cn (K.L.); zhongm@epri.sgcc.com.cn (M.Z.)

<sup>2</sup> Qingdao Power Supply Company of State Grid Shandong Province Electric Power Company, Qingdao 266001, China; liguoshi@163.com

\* Correspondence: ai15222883228@163.com

**Abstract:** Under the dual carbon strategy, with the frequent occurrence of extreme weather and the further increase in uncertainty of multi-user behavior, it is urgent to improve the stability of the heating systems and reduce heating energy consumption. Aiming at the problem of fault-disturbance control of the multi-user heating network in an integrated energy system, this paper proposes a novel analysis method of resistance–capacitance reactance based on the circuit principle to construct a dynamic thermal-power-flow model of the whole link of the multi-user heating network and analyze the fault-disturbance propagation characteristics of the heating network by this model. It shows that the difference in disturbance characteristics of different users in a multi-user heating network mainly depends on the characteristics of the heating pipeline between the heat user and the heat source, which provides a necessary basis for formulating intelligent control strategies against fault disturbance. Finally, taking a typical daily outdoor temperature in Beijing in winter as an example, this paper compares two different heating strategies and the blocker installation methods of the multi-user heating network to obtain a better heating strategy under actual conditions. Considering the heating fault disturbance, this paper proposes a novel intelligent heating strategy whose heating temperature will decrease during the fault-disturbance time, with an energy saving of about 16.5% compared with the heating strategy under actual conditions during the same period.

**Keywords:** heating network; resistance-capacitance reactance; thermal power flow; fault disturbance; intelligent control



**Citation:** Jin, L.; Shi, L.; Li, D.; Liu, K.; Zhong, M.; Pang, J. Anti-Disturbance Integrated Control Method and Energy Consumption Analysis of Central Heating Systems Based on Resistance–Capacitance Reactance. *Sustainability* **2023**, *15*, 12496. <https://doi.org/10.3390/su151612496>

Academic Editors: Ahmad Arabkoohsar and Meisam Sadi

Received: 8 June 2023

Revised: 24 July 2023

Accepted: 27 July 2023

Published: 17 August 2023



**Copyright:** © 2023 by the authors. Licensee MDPI, Basel, Switzerland. This article is an open access article distributed under the terms and conditions of the Creative Commons Attribution (CC BY) license (<https://creativecommons.org/licenses/by/4.0/>).

## 1. Introduction

In the context of the dual carbon strategy, proposing and developing an integrated energy system is an effective way to improve energy structure and energy efficiency, which can balance renewable energy consumption and comprehensive utilization efficiency through multi-energy complementation and multi-energy flow synergy, and lay the foundation for building a clean, low-carbon, safe and efficient energy system [1]. However, under the premise of meeting the diversified energy demand of users such as cooling, heating, and electricity, the integrated energy system makes for the deep integration and interaction of different energy flow systems such as the traditional power system, thermal system, and gas system, which greatly increases the complexity of modeling analysis and optimization regulation of integrated energy systems [2]. With the frequent occurrence of extreme weather and the increase in uncertainty in the behavior of multi-user subjects, the fault disturbances generated by different energy flow subsystems will be separated from a single subsystem and generate cross-system propagation and evolution, further increasing the difficulty of intelligent regulation and affecting the stable operation of integrated energy systems.

To study the anti-disturbance characteristics of the heating network, and then improve the heating strategy of the heating network to obtain a more flexible and energy-saving intelligent heating strategy, dynamic modeling of the heating network is the primary prerequisite. Luo et al. [3] constructed a novel model for propagating clean heating acceptance, ACHRA, based on the concentration of heat users, providing guidance for heat network modeling. Based on the thermal resistance theory, Dai et al. [4] modeled the heat source, heat exchanger, piping, and heat load of the electric heating system from the perspective of thermoelectric analogy, giving two different piping models that are important for the model construction of the heating network. It shows the direction for the construction of the next pipeline dynamic model of the heating network. Ge et al. [5] constructed an overall dynamic heat-flow model of the heating system from the heat source to the user by dynamically modeling the key components based on the standardized thermal resistance defined by the inlet-temperature difference. A foundation is laid for the application of the analogous circuit method to the construction of heating network models. Jiang et al. [6] designed a modeling approach for district heating (DH) networks based on a compact model of the data. However, the control equations of this method are more complex and have more intermediate parameters. Zhao et al. [7] developed a dynamic characteristic model for analyzing the nonlinear characteristics of heating networks based on a modified Elman neural network. But the solution of this modeling method is quite difficult. In summary, the models constructed by the current dynamic modeling of heating networks are relatively complex, with many intermediate parameters, and the extensibility and compatibility of the models are low.

For different energy flow subsystems in an integrated energy system, the concept and type of fault disturbance do not have the same meaning. Take the centralized heat system on the customer side as an example; it is a multi-input and multi-output system with a large scale, large latency, and high coupling of each variable. With the increasing complexity of the heating network, there will be more and more heating disturbances and faults [8] in the heating network. The heating disturbances and faults in the heating network will cause the indoor temperature to be substandard on the user side and increase the energy consumption of the heating network, so it is necessary to adopt more advanced and intelligent heating strategies in order to reduce the effects of heating disturbances and faults in the heating network. Huang et al. [9] pointed out that China's centralized heat supply industry is developing rapidly. Taking advantage of advanced information and communication technology and Internet platforms to promote intelligent energy production, interconnection and interoperability of various energy-flow networks, and collaborative transformation of multiple energy forms is an important direction for the transformation and upgrading of the energy industry. To cope with uncertain thermal disturbances on the user side, Yang et al. [10] integrated hybrid mechanisms and deep learning methods into a novel heating-load model (BHLP-UN model). Compared with the conventional model which only considered the meteorological factors and the thermal inertia, the mean absolute percentage error of this model decreases by 53.512~65.338% for different types of heat users and the annual load could decrease to 26.501~28.572%. Liu [11] considered the stabilization of a thermal system with input delay and control matching disturbances, transformed the input delay term into a first-order hyperbolic equation to obtain a cascaded PDE system, and improved the stability of the heating system in the face of disturbances by applying active disturbance-suppression control methods in real time to estimate the disturbances and then designing feedback control. Based on the LADRC control algorithm, Jin et al. [12] proposed a design scheme for an energy-saving heating control system by combining ZigBee wireless communication technology, M-Bus bus transmission technology, and Web configuration software, which achieved automatic room temperature regulation in the face of heating disturbances. Thenmozhi M. et al. [13] studied hybrid controllers, i.e., PID-based IMC controllers, showing that many more complex factors contribute to the temperature control capability of the heating system under disturbances and delays than other controllers. Wei et al. [14] investigated the

ability of model predictive control (MPC) to achieve a balance of energy efficiency, thermal comfort, and air quality, minimize peak load demand and maximize the production of renewable energy in buildings, and improve the flexibility of heating systems in response to heating disturbances. Edward O'Dwyer et al. [15] devised a novel spatiotemporal filtering technique for estimating disturbances and combined it with a meta-heuristic search method to propose a method for deriving low-order models from data suitable for use in optimization-based MPC strategies to improve the flexibility of heating systems.

Improving the overall anti-disturbance capability of the heating network, improving its flexibility and energy efficiency, further improving the heating strategy [16], and gradually realizing smart heating [17–19] are the main directions for the future development of the heating network. For this goal, many scholars have made attempts in this regard. Jelger Jansen et al. [20] proposed a rule-based controller (RBC) control method for the district heating (DH) network that considers the system as a whole (including the heating demand side) and incorporates important nonlinearities and all types of flexibility into the MPC's controller model to improve the heating-network prediction capability and flexibility. Ju et al. [21] proposed and established a model predictive control strategy based on RBF neural networks, which improved the control effect and reduced the energy consumption in the heating process while improving the comfort of heat users. Ge et al. [5] proposed a variety of heating strategies developed based on an iterative approach for hourly mass regulation of primary heating networks, and the proposed user-following heating strategy section saved 25.27% energy compared to the all-day heating strategy, and further proposed five different heating strategies, i.e., all-day constant heating, inverted triangular, step, trapezoidal, and parabolic, to achieve energy savings in the practical application of heating systems operation. Valentin Kaisermayer et al. [22] presented two control methods for interconnected DH networks that optimized the supply and demand sides to reduce CO<sub>2</sub> emissions. On the supply side, an optimization-based energy management system defined operating strategies based on demand forecasts. On the demand side, the operation of customer substations was influenced in favor of supply using demand-side management. Elena N. Desyatirikova et al. [23] proposed a heating control system containing three temperature controllers, which effectively improved the rationality and energy efficiency of the heating network control strategy. Zheng et al. [24] proposed a variable differential-pressure heating-network control strategy based on end-load monitoring, and the energy consumption of the proposed heating strategy can be reduced by 34.27% compared with the traditional constant differential-pressure control strategy. The above-mentioned multi-type heating strategies for multi-user heating networks focus on a simplified model of the heating network or focus on smart heating from the control perspective, whose overall objectives mainly include user comfort and satisfaction, system safety and reliability, efficient energy utilization, and low-carbon and clean economy. However, with the further recommendation of regional integrated energy systems and the construction of new power systems, exploring the variability of electric and thermal loads of different users and the feasibility of [25,26] integration is the key to the efficient, flexible, and stable operation of future integrated energy systems, and electric and thermal interaction makes the study of the evolution of fault disturbances generated on the user side in this system and the propagation characteristics of cross-systems more urgent, taking into account the propagation of fault disturbances in heating systems. Intelligent control strategies for the propagation of fault disturbances in heating systems need more theoretical basis and practical application.

However, the models constructed in the current dynamic modeling of heating networks and heating strategy optimization are relatively complex, with many intermediate parameters and low model extensibility and compatibility. At the same time, the current modeling methods have difficulty in accurately following the load fluctuations on the customer side, and the response speed is slow, making it difficult to quantitatively analyze the stochastic behavior of customers. To address the research gap mentioned above, this paper constructs a dynamic thermal power flow model of the whole link of the multi-user heating network in the integrated energy system and analyzes the fault-disturbance propagation

characteristics of the heating network by this model; its key contributions are summarized as follows:

1. This paper proposes the resistance–capacitance reactance method based on the circuit principle to model and analyze the whole link of the heating network.
2. This paper analyzes the fault-disturbance propagation characteristics of the heating pipes and multi-user heating network, which provides a necessary basis for formulating intelligent control strategies against fault disturbance in the integrated energy system.
3. This study compares two different heating strategies and the blocker installation methods of the multi-user heating network when the outdoor temperature varies and obtains a new intelligent heating strategy that can effectively resist disturbance.

The sections of this paper are structured as follows: Section 2 constructs the dynamic thermal-power-flow model of the whole link of the multi-user heating network. On this basis, Section 3 analyzes the fault-disturbance propagation characteristics of the multi-user heating network by the model. Subsequently, Section 4 studies the heating strategy of a multi-user heating network in practical situations and proposes the corresponding smart heating strategy against fault disturbance. Lastly, the research conclusion is summarized in Section 5.

## 2. Dynamic Thermal-Power-Flow Model for Multi-User Heating Networks

The integrated energy system contains two categories of electrical network and heating network. The access to various types of electrical and thermal conversion devices in the power grid and heat network further integrates the electrical and thermal dual networks, which increases the difficulty and complexity of fault analysis in integrated energy systems. Among these networks, the integrated heating network intertwined for multiple sources and multiple users, as shown in Figure 1, is a typical complex network with asynchronous delays and multiple device coupling. The heat source uses high-temperature steam, electric heating, and electric heat pumps to heat the hot-side work mass in the heat exchanger station, and the heated hot-side work mass of the heat exchanger station heats the low-temperature work mass in the heat exchanger, and the heated low-temperature work mass is transported through heating pipes of different lengths and enters different radiators, where it exchanges heat with indoor air to achieve heating for different types of users. The work mass after heat exchange in the radiator is then transported by the return pipeline to the low-temperature side inlet of the heat exchanger.

Due to the characteristics of multi-user participation, multi-device coupling, and strong asynchronous delays in heating networks, the overall modeling and analysis of multi-user participation in heating networks is the basis for analyzing the propagation of fault disturbances. In this section, based on the differential equations of the heat transfer process and the equivalent circuit method in the circuit principle, the heat transfer and transport processes of heat exchangers, heat transfer pipes, and radiators on the user side in the integrated heating network are simplified and analyzed, respectively, and the dynamic thermal-power-flow model is constructed to study the heat-transfer state in the multi-user heating network, and to analyze the propagation and evolution law of fault disturbance in the multi-user heating network.

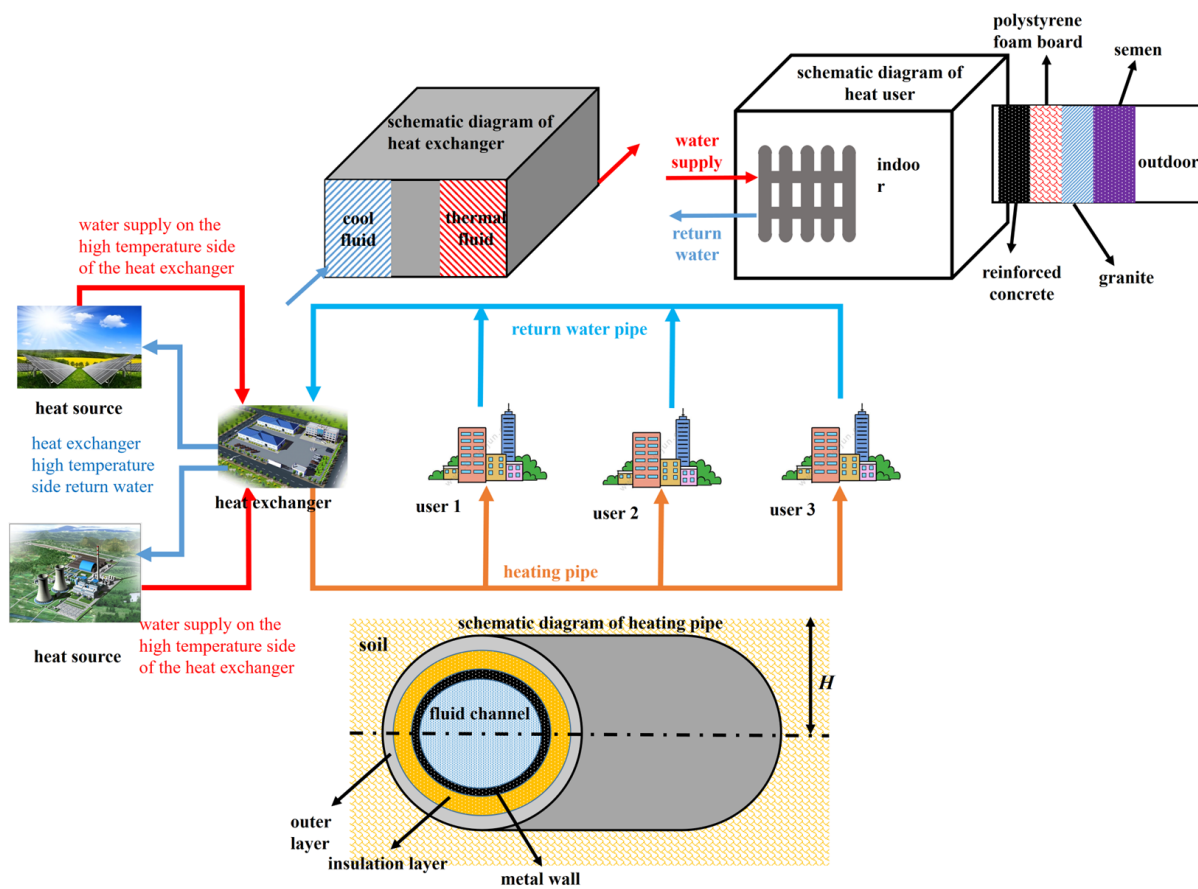


Figure 1. Schematic diagram of multi-user integrated heating network.

### 2.1. Dynamic Thermal-Power-Flow Model for Different Heat-Transfer Processes

For the heating network containing different users in the district integrated energy system shown in Figure 1, the heat exchanger, the mass-transfer pipeline and the radiator on the user side are the key equipment and important links of the integrated energy-supply heat network. Therefore, integrated modeling of the physical processes of each link and equipment is required. For heat-exchange equipment in heat-transfer stations, the main dynamic heat-transfer processes need to consider the dynamic transfer and storage characteristics of the heat-transfer process. According to the dynamic heat-transfer process of the heat exchanger and its thermal-power-flow model [27], it is known that the dynamic heat-transfer process of the heat exchanger can be expressed as:

$$C_{wall} \frac{\partial T_{wall}}{\partial t} = \frac{T_{h,in}(t) - T_{wall}(t)}{R_h} - \frac{T_{wall}(t) - T_{c,in}(t)}{R_c} \quad (1)$$

where  $T_{wall}$ ,  $T_h$ ,  $T_c$  are the heat-exchanger metal wall, hot-side fluid, and cold-side fluid local temperature;  $T_{h,in}$  and  $T_{c,in}$  are the inlet temperature of the hot fluid and cold fluid, respectively;  $C_{wall}$  is the equivalent heat capacity of the heat-exchanger wall.  $R_h$  and  $R_c$  are the standard thermal resistance of heat transfer between hot-side fluid, cold-side fluid, and the heat-exchanger wall, respectively. The specific calculation of expressions for [27]:

$$R_h = \frac{1}{G_h(1 - e^{-NTU_1})} \quad (2)$$

$$R_c = \frac{1}{G_c(1 - e^{-NTU_2})} \quad (3)$$

where,  $NTU_1 = \phi k_h A / G_h$ ,  $NTU_2 = \phi k_c A / G_c$ .  $\phi$  is the correction factor of this heat exchanger.  $G_h$  and  $G_c$  denote the heat-capacity flow rate of the fluid on the hot side and cold side, respectively, which is the product of mass flow rate and constant pressure-specific heat capacity.  $k_h$  and  $k_c$  denote the convective heat-transfer coefficients between the hot-side fluid, cold-side fluid and the heat-exchanger wall, respectively, and  $A$  is the heat-transfer area of the heat-exchanger wall [28].

According to the dynamic heat-transfer process of the above heat exchanger and by analogy with the RC circuit in the resistance–capacitance reactance principle, a dynamic thermal-power-flow model of the heat-transfer process of the heat exchanger in a multi-user heating network can be obtained by analogous electrical analysis, as shown in Figure 2, which contains two equivalent thermal resistances and one equivalent thermal capacity, demonstrating the heat-transfer process between the fluid and the metal wall inside the heat exchanger, i.e., part of the heat from the hot fluid is transferred to and absorbed by the heat-exchanger wall, and part of the heat is transferred to and absorbed by the cold fluid.

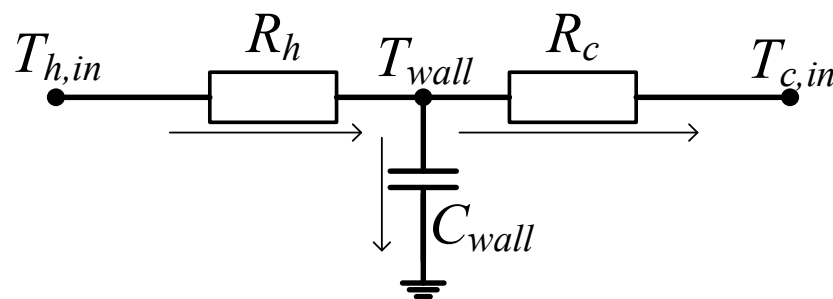


Figure 2. Dynamic thermal-power-flow model of heat exchanger in heat-exchange station.

In addition, in a multi-user integrated heating network, the carrier mass of heat needs to be circulated and transported through the water supply and return piping, which plays a key role in the propagation of fault disturbances in the system. When the high-temperature work fluid flows in the pipeline, it will dissipate heat through the pipe wall to the surrounding soil, etc., causing energy loss, and at the same time, due to the finite heat capacity and the finite velocity of the fluid flow process, a certain delay characteristic from the heat exchange station to different users, similar to the current flowing through the inductor in an AC circuit, will produce hysteresis. Therefore, in this paper, a dynamic thermal-power-flow model for water supply and return pipes is constructed by analyzing the pipe-heat-dissipation model [27], and the dynamic process can be expressed as:

$$C_p \frac{\partial T_p}{\partial t} = \frac{T_{d,in}(t) - T_p(t)}{R_d} - \frac{T_p(t) - T_s(t)}{R_s} \quad (4)$$

where  $T_s$ ,  $T_p$  and  $T_d$  denote the soil, pipe wall, and fluid local temperature inside the pipe, respectively.  $C_p$  denotes the equivalent heat capacity of the wall of the heating pipe;  $T_{d,in}$  indicates the inlet temperature of the fluid in the pipeline;  $R_d$  denotes the standard thermal resistance between the heating fluid inside the pipe and the metal wall of the pipe.  $R_s$  denotes the standard thermal resistance of heat transfer between the pipe wall and the outer soil, which can be expressed, respectively, as [27]:

$$R_d = \frac{1}{G_d(1 - e^{-NTU_3})} \quad (5)$$

$$R_s = \frac{1}{\sum_{i=1}^3 \frac{\delta_i L_2}{\lambda_i A_i}} \quad (6)$$

where,  $NTU_3 = k_d A_d / G_d$ ,  $G_d$  denotes the heat-capacity flow of the fluid inside the pipe, which is the product of mass flow rate and specific heat.  $k_d$  denotes the convective heat-

transfer coefficient inside the pipe.  $\delta_i$  ( $i = 1, 2, 3$ ) denotes the thickness of the insulation, shell, and soil of the heating pipe.  $\lambda_p$  denotes the thermal conductivity of the pipe wall metal.  $\lambda_i$  ( $i = 1, 2, 3$ ) denotes the thermal conductivity of the insulation, shell, and soil.  $A$  denotes the heat-transfer area of the inner wall of the pipe.  $L_2$  indicates the length of the pipe.

By comparing Equations (1) and (4), which have the same expression form, the same analogy with the RC circuit in the resistance–capacitance reactance principle, and the dynamic thermal-power-flow model of the heat-transport process of the heating pipes in the multi-user heating network can be obtained by analogous electrical analysis, as shown in Figure 3, which includes two standard thermal resistances and an equivalent heat capacity, reflecting the dynamic loss of the enthalpy flow of the work mass in the pipe transport process. That is, part of the heat of the fluid volume is absorbed by the pipe wall and the other part of the heat is dissipated into the external environment and absorbed by the soil.

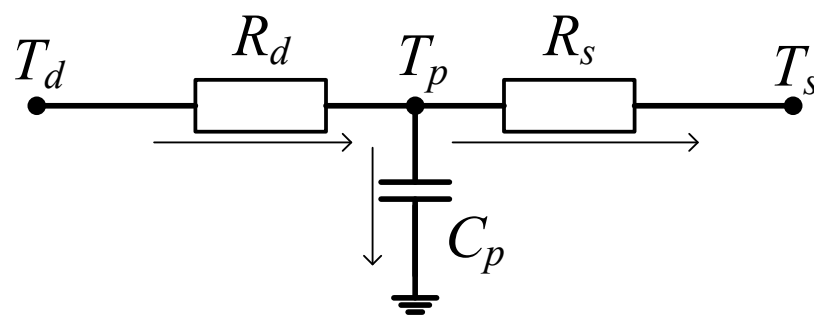


**Figure 3.** Local model of thermal power flow of working fluid-transport pipeline.

The user side in the heat dissipation equipment mainly refers to the radiator, the device capable of transferring heat from the high-temperature mass inside the radiator to the user's room, and is the terminal equipment in the heating network. In integrated energy systems, multi-user heating-network fault perturbations include uncertainties and randomness caused by user behavior, whose propagation characteristics, the variability of the respective room temperatures, and the associated anti-disturbance heating strategies can have a large impact on the overall scheduling and operation of the system. Therefore, it is crucial to prepare radiator-heat dynamic transfer models that portray and describe the metered and user behavior.

Since the radiators are arranged directly on the user side, the room can be equated to a hexahedron, and it is assumed that the air is fully exchanged at all locations in the room with uniform temperature distribution, while ignoring the influence of indoor appliances, etc. on the heat-exchange process. Since the temperature change in the room depends on the heat dissipation of the radiator and the heat exchange between the building and the outdoor environment, the heat-capacity characteristics of the indoor air and the heat storage and thermal-protection capacity of the building walls need to be considered. Analyzing the radiator and the building wall separately, the dynamic thermal-power-flow model of the water supply and return piping [27] is constructed in this paper by invoking the dynamic model of the heat exchanger and the one-dimensional multilayer wall transient thermal conductivity control equation, whose dynamic process expression is:

$$C_r \frac{\partial T_r}{\partial t} = \frac{T_{d,in}(t) - T_r(t)}{R_{d,in}} - \frac{T_r(t) - T_a(t)}{R_a} \quad (7)$$

$$C_a \frac{\partial T_a}{\partial t} = \frac{T_r(t) - T_a(t)}{R_a} - \frac{T_a(t) - T_{sa}(t)}{R_{sa}} \quad (8)$$

where,  $T_a$ ,  $T_r$ ,  $T_{sa}$ ,  $T_d$  indicate the instantaneous temperature of indoor air, radiator metal wall, outdoor air, and internal fluid of the radiator;  $T_{d,in}$  indicates the fluid-inlet temperature inside the radiator;  $R_{d,in}$ ,  $R_a$ ,  $R_{sa}$ , respectively, indicate the inside of the radiator, the outside

of the radiator and the standard thermal resistance between indoor air and outdoor air; the calculation formulas are [27]:

$$R_{d,in} = \frac{1}{G_d(1 - e^{-NTU_4})} \quad (9)$$

$$R_a = \frac{1}{k_a A_a} \quad (10)$$

$$R_{sa} = \sum_{i=1}^4 \frac{\delta_i L}{\lambda_i A} + \sum_{i=1}^2 \frac{L}{h_i A} \quad (11)$$

where,  $NTU_4 = k_d A / G_d$ ,  $k_d$ ,  $k_a$  denote radiator wall and internal fluid and convective heat transfer coefficients with indoor air, respectively.  $C_a$  denotes the equivalent heat capacity of indoor air.  $\lambda_i$  and  $\delta_i$  ( $i = 1, 2, 3, 4$ ) denote the thermal conductivity and thickness of each insulation layer.  $\lambda_w$  denotes the thermal conductivity of the radiator walls.  $h_{in}$  and  $h_{out}$  denote the indoor and outdoor heat-transfer coefficients.

Comparing Equations (1) and (4) and Equations (7) and (8), the same analogy with the RC circuit in the resistance–capacitance reactance principle, and the dynamic thermal-power-flow model of the dynamic process of heat transfer between radiators and indoor air in a multi-user heating network can be obtained by analogous electrical analysis, as shown in Figure 4, which contains two equivalent heat capacities and three standard thermal resistances, fully reflecting the heating mass into the building. After that are the heat-transfer process and heat-capacity delay characteristics. That is, part of the heat of the fluid inside the radiator is absorbed by the metal wall of the radiator, and part of the heat is transferred to the air, in which part of the heat is absorbed by the indoor air and the remaining heat is transferred to the outdoor air.

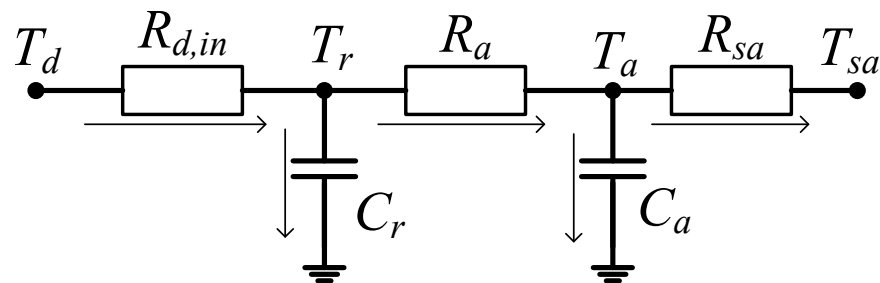


**Figure 4.** Dynamic thermal-power-flow model considering radiator and building heat users.

## 2.2. Dynamic Thermal-Power-Flow Model for Multi-User Heating Networks

According to the dynamic thermal-power-flow model of different heating links or equipment in the multi-user heating network, the equipotential points in the model can be connected, thus obtaining the overall dynamic thermal-power-flow model from the heat source to the user as shown in Figure 5. In this figure,  $T_{h,in}$  is the inlet temperature of the water on the hot side of the heat exchanger,  $T_{c,in}$  indicates the inlet temperature of the water on the cold side of the heat exchanger,  $T_{a1}$ ,  $T_{a2}$ ,  $T_{a3}$  indicate the indoor temperature of different users,  $T_s$  indicates the soil temperature,  $T_{sa}$  indicates the outdoor temperature, and it should be noted that since the length of the heating pipes between different users and the heat source is different, the size of the thermal resistance and the delay characteristics of the three pipes are not the same.

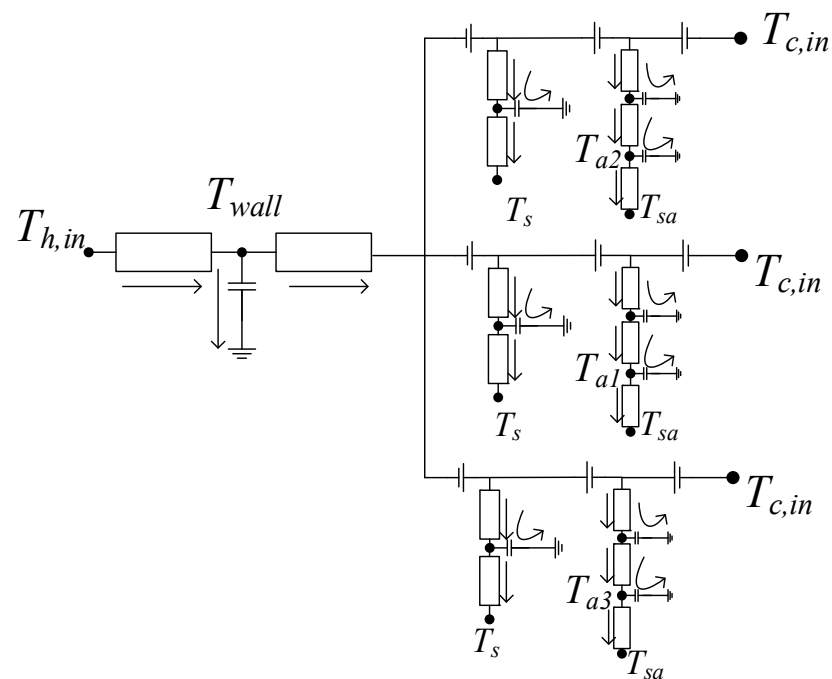


**Figure 5.** Dynamic thermal-power-flow model of heating network [5].

### 2.3. Validation of the Dynamic Thermal-Power-Flow Model for the Heating Network

The dynamic thermal-power-flow model of a multi-user heating network was built in Section 2.2 based on the analog circuit method by MATLAB. To ensure the accuracy of the results simulated by this model, this section takes the heat-exchanger model and the pipeline model as examples, providing the validation of these two models by numerical simulation through the software FLUENT. Figure 6 shows the two numerical models built by FLUENT: (a) Heat-exchanger model; (b) Pipeline model. The length of the heat exchanger and the pipeline is appropriately shortened to simplify the calculation, which is 1.5 m and 30 m, respectively. The flow rate of fluids in the heat exchanger and pipeline is set to 0.5 m/s.

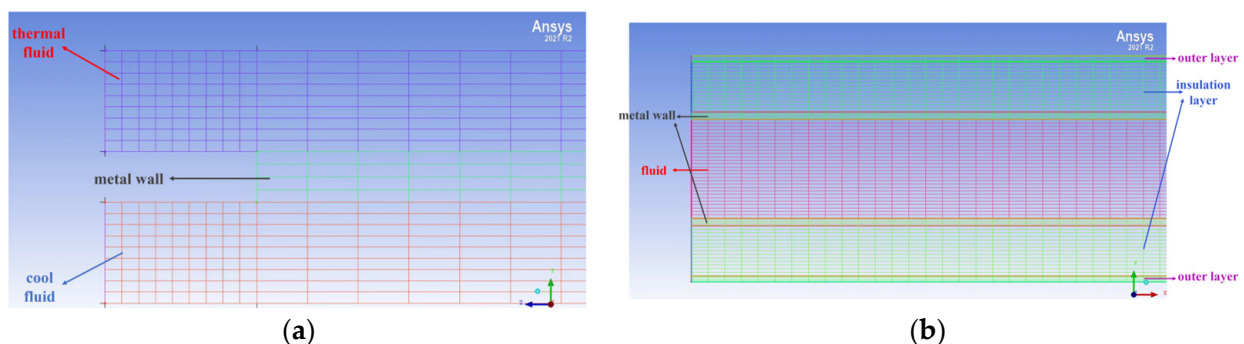


**Figure 6.** Two numerical models: (a) Heat-exchanger model. (b) Pipeline model.

The dynamic thermal-power-flow model and fluent model are applied to simulate the heat-transfer process in the heat exchanger and heat transport in the pipeline. The outlet temperature of the cold-side water of the exchanger and the pipeline outlet temperature were obtained by the two models, respectively. The comparison results are shown in Figure 7. At the initial time, the inlet temperature of the hot-side water in the exchanger is set to 90 °C, the cold-side water inlet temperature is 50 °C, and the initial temperature of the heat-exchanger wall and the remaining water is set to 70 °C. From Figure 7a we can see that the outlet temperatures of cold-side water in the heat exchanger calculated by the two

models are almost consistent. For the pipeline model, at the initial time, the temperature of the pipe inlet and the pipe wall is set to 70 °C, and the soil temperature is −5 °C. Figure 7b shows the calculation results of temperature change and delay characteristics of the pipeline outlet when the pipeline inlet temperature steps from 70 °C to 60 °C at the 0th s. The pipeline outlet temperature calculated by the thermal-power-flow model has good agreement with the result obtained by the fluent model, and the temperature-change propagation time is a few seconds later than the fluent model due to the segmentation method in the thermal-power-flow model of the pipeline, ignoring the temperature gradient inside the segment. The comparison results show that the proposed thermal-power-flow model for the heat network has high reliability in predicting the temperature and heat-disturbance propagation characteristics of the heat network.

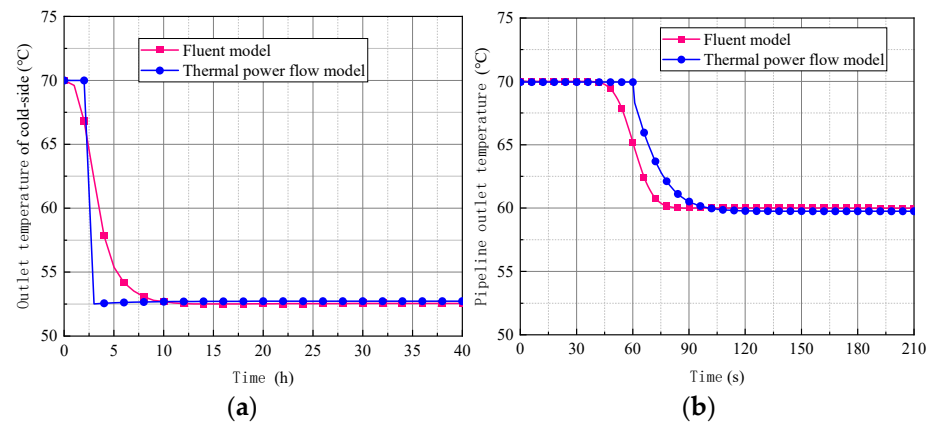


**Figure 7.** Comparison results of the thermal-power-flow model and fluent model: (a) Heat-exchanger model. (b) Pipeline model.

### 3. Fault-Disturbance Propagation Characteristics of Multi-User Heating Networks

Due to the different lengths of the heating pipes connecting each user to the heat source, the multi-user heating network will inevitably come to greater variability in the propagation-evolution characteristics of the heating fault disturbance at the heat source side in the transmission process. Moreover, the flow of heating fluids in the heating pipes will also produce different heat losses, which will lead to large differences in the heat transfer to the user side at the same heating temperature and outdoor temperature. In the face of different heating demands and uncertainty of fault disturbance of multiple users, it is necessary to consider the fault-disturbance propagation characteristics of different lengths of heating pipes and the difference of fault propagation characteristics of heating network, as well as the heat loss of different lengths of heating pipes and the difference of indoor temperature of users due to heat loss, to develop individual wisdom strategies for anti-fault disturbance.

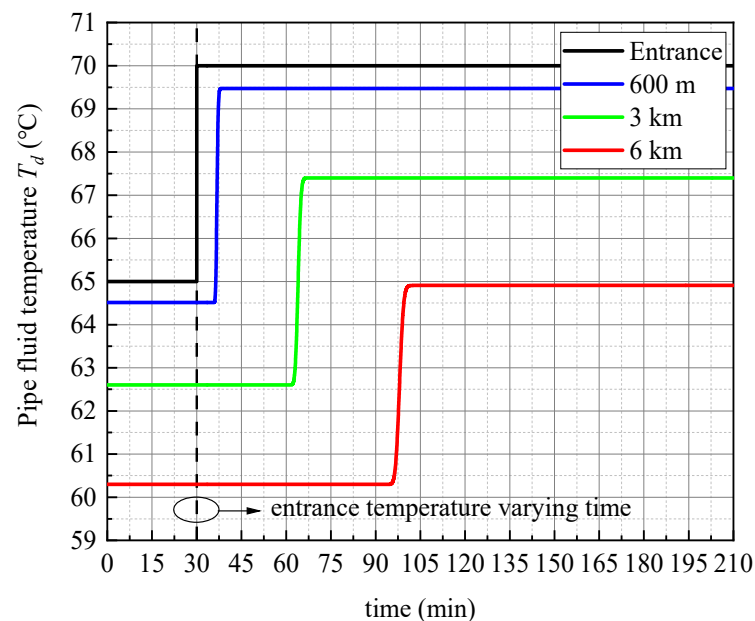
#### 3.1. Fault-Disturbance Propagation Characteristics of Heating Pipes

This subsection will build on Section 2.1 and combine the idea of segmental study with the thermal-power-flow model obtained in Section 2.1. The process of the change of the outlet temperature of the heating pipes of different lengths in the face of the step of the inlet-fluid temperature is analyzed and studied, and the operating and structural parameters of the heating pipes are given as shown in Table 1.

**Table 1.** Operation and structural parameters of heat-supply pipeline.

Name	Value	Name	Value
Distance between pipeline and ground surface/m	0.8	Carbon steel wall thickness/m	0.0045
PE pipe shell thickness/m	0.0035	Pipe O.D./m	0.059
Thickness of rigid polyurethane outer layer/m	0.03	Fluid flow rate/(m/s)	1.94

The fluid-inlet temperature of the heating pipe is initially set to 65 °C, and the temperature at the outlet of the heating pipe is not the same for different lengths at this time; as shown in Figure 8, the outlet temperature of the heating pipe with a length of 600 m is about 64.5 °C, the outlet temperature of the heating pipe with a length of 3000 m is about 62.6 °C, and the outlet temperature of the heating pipe with a length of 6000 m is 60.3 °C. Under the operating conditions and structural parameters given in Table 1, the heat loss per kilometer of the heating pipeline is about 0.81 °C. The heat loss caused by pipeline transportation makes the indoor temperature of users with different distances from the heat source in the multi-user heating network vary even when they face the same outdoor temperature.

**Figure 8.** Outlet temperature change after step change of inlet temperature of heat supply pipes with different lengths.

When the fluid temperature at the inlet of the heating pipe steps, the fault-propagation characteristics of different lengths of heating pipes also show some differences. As shown in Figure 8, the fluid temperature flowing into the heating pipe steps from 65 °C to 70 °C at the 30th min, and the disturbance-response time for different lengths of heating pipes is approximately equal to the time required for the fluid to flow from the inlet to the outlet of the heating pipe. The perturbation time is 6.1 min for a 600 m-length heating pipe, 32.4 min for a 3000 m-length heating pipe, and 65.7 min for a 6000 m-length heating pipe. There is also a slight variability in the time required between the change in outlet temperature and the new steady state of the outlet temperature for different-length heating pipes. The time required for a 600 m-length heating pipe to reach a new steady state at the outlet fluid temperature is about 2 min; the time required for a 3000 m-length heating pipe to reach a new steady state at the outlet fluid temperature is about 3.4 min; the time required for a 6000 m-length heating pipe to reach a new steady state at the outlet fluid temperature is

about 4.8 min. The time required for different lengths of heating pipes from the beginning of the change in outlet temperature to the new steady state is positively related to the length of the pipes, but the difference in values is not significant.

The time required to start the change of the outlet temperature of the heating pipe with a length of 600 m accounts for 75.3% of the time required for the change of the outlet temperature of the heating pipe; the time required to start the change of the outlet temperature of the heating pipe with a length of 3000 m accounts for 90.5% of the time required for the change of the outlet temperature of the heating pipe; the time required to start the change of the outlet temperature of the heating pipe with a length of 6000 m accounts for 93.2% of the time required for the process of temperature change at the outlet of the heating pipe. It shows that the delay in heating the pipe mainly comes from the time required for the flow of fluid in the heating pipe, and the longer the length of the pipe, the greater the proportion of the delayed response time of heating the pipe to the time required for the whole temperature change process.

### 3.2. Fault-Disturbance Propagation Characteristics of Multi-User Heating Networks

This subsection will build on Section 2.2 and combine the ideas of the segmental study with the dynamic thermal-power-flow model of a multi-user heating network obtained in Section 2.2. The delay in the indoor temperature of heat consumers with different lengths of heating pipes is analyzed and investigated in the case of a step in the temperature of the inlet fluid (heating temperature) facing the hot side of the heat exchanger. Now given the plate counterflow heat exchanger and radiator operating and structural parameters as shown in Tables 2 and 3, and the heating pipe structural parameters as shown in Table 1, the parameters are set so that the fluid flow velocity in the heating pipe is about 1.94 m/s. The number of users is assumed to be 3, and the lengths of heating pipes are 600 m, 3000 m, and 6000 m, respectively.

**Table 2.** Operation parameters of heat exchanger.

Name	Value	Name	Value
Length/m	15	Fluid pipe thickness/m	0.01
Aluminum plate thickness/m	0.005	Fluid flow rate/(m/s)	1
Fluid pipe width/m	2		

**Table 3.** Operation parameters of rooms and radiators.

Name	Value	Name	Value
Room size/m × m × m	10 × 8 × 3	Cement mortar thickness/m	0.02
Granite thickness/m	0.02	Polyethylene foam board thickness/m	0.05
Reinforced concrete thickness/m	0.28	Number of cast iron radiator pieces	30

Keeping the outdoor temperature constant at 3 °C, the simulation results are shown in Figure 9. When the heating temperature is 70 °C, there are slight differences in the indoor temperatures of users connected by different lengths of heating pipes: the indoor temperature of the user with a pipe length of 600 m is 26.6 °C; the indoor temperature of the user with a pipe length of 3000 m is 25.8 °C; and the indoor temperature of the user with a pipe length of 6000 m is 24.9 °C. The temperature difference is caused by the heat loss of fluid in the heating pipe as it flows into the pavilion. At the 30th min, the heating temperature has a step of 70 °C to 50 °C: the time required to start the change of indoor temperature for the heat customer with a pipe length of 600 m is 7.2 min; the time required to start the change of indoor temperature for the heat customer with pipe length 3000 m is 34.3 min; the time required to start the change of indoor temperature for the

heat customer with pipe length 6000 m is 68.8 min. Compared with the pipe-disturbance characteristics in the previous subsection, the time required from the change of pipe-inlet temperature to the change of pipe-outlet temperature accounts for 84.7%, 94.5%, and 95.5% of the heating-network disturbance response time, respectively. It can be concluded that the longer the pipe length is, the greater the proportion of the delayed response time of the pipe to the delayed response time of the heating network.

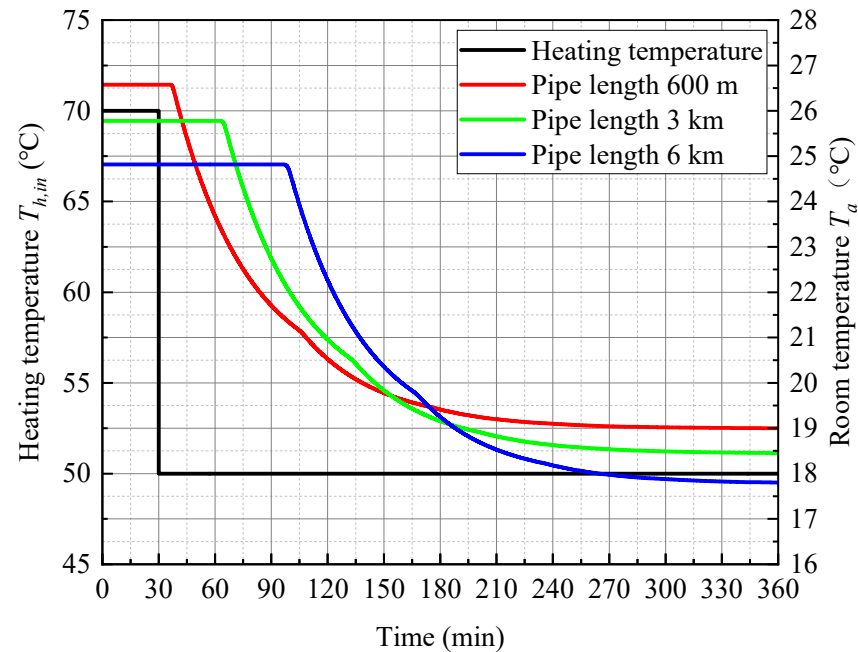


**Figure 9.** Change of indoor temperature of different heating pipes after step change of heating temperature.

The time required for the three users to reach a new steady state from the beginning of the indoor temperature change is 226.5 min for the user with a pipe length of 600 m, 250.3 min for the user with a pipe length of 3000 m, and 276.5 min for the user with a pipe length of 6000 m. The time required for the three users to restabilize the indoor temperature from the beginning of the indoor temperature change is governed by the pipe length; the larger the pipe length, the larger the pipe delay will be in the delay of the whole heating network.

It is concluded that in a multi-user heating network, different lengths of heating pipes lead to differences in temperature at the outlet of the pipes and thus in indoor temperature. For a multi-user heating network, the delayed response time of its different users depends more on the length of the heating pipes.

#### 4. Analysis of Intelligent Heating Control Strategies for Anti-Disturbance of Multi-User Heating Networks

This section explores the practical heating strategies for multi-user heating networks and the smart heating strategies that should be adopted by heating networks in the face of heating disturbances, as the outdoor temperature varies when the heating network is supplying heat to the building and due to the living behavior of users.

##### 4.1. Heating Strategy of Multi-User Heating Network under Actual Conditions

During the heating season, the outdoor temperature is constantly changing with time. In this section, we will take the temperature change of a day in the winter heating season in Beijing as an example, whose temperature changes with time as shown in Figure 10, and explore the actual heating strategy of the multi-user heating network and the smart heating strategy in the face of heating disturbances.

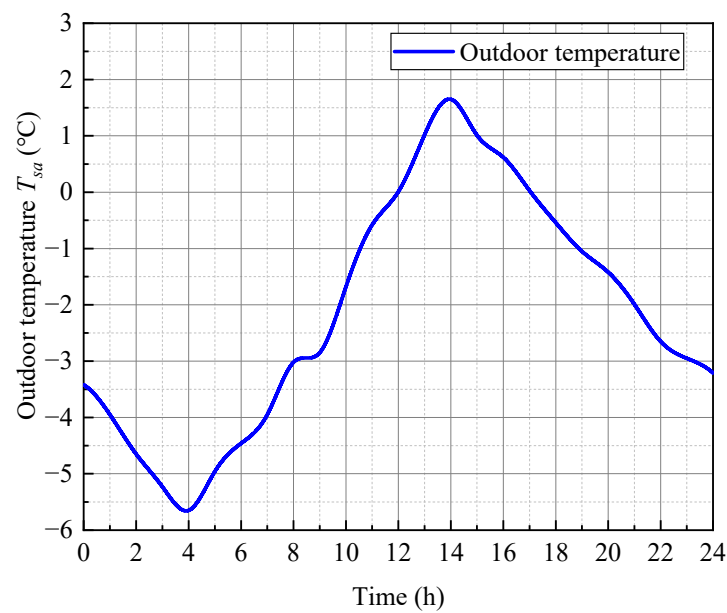


**Figure 10.** Outdoor temperature change of a day (23 December 2021) in Beijing heating season.

A dynamic model was constructed with the operational and structural parameters of the multi-user heating network simulated in Section 3.2 to analyze the difference in indoor temperature under the effect of the same outdoor temperature trend and the same heating temperature. The outdoor temperature is shown in Figure 10. The heating temperature is constant at 65 °C, and the indoor temperature-variation trend of the three users is shown in Figure 11. According to the indoor temperature-change trend shown in Figure 11, it can be concluded that the indoor temperature-change trend of each user in the multi-user heating network is the same as the outdoor temperature-change trend; the indoor temperature level of each user decreases with the increase in pipe length.

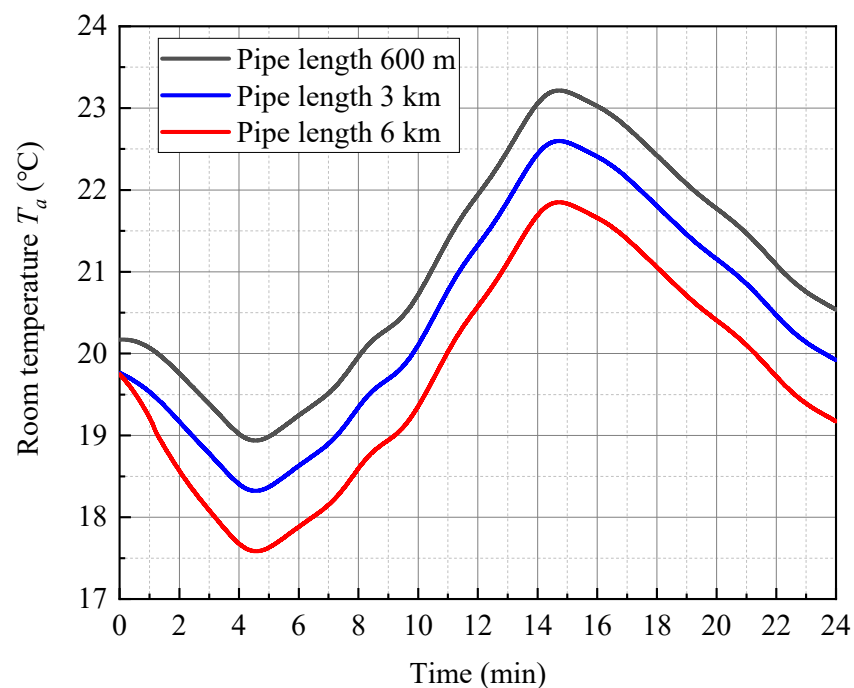


**Figure 11.** Indoor temperature change of each user in multi-user heating network when the heating temperature is 65 °C.

According to the analysis in Section 3.2, the fault-propagation characteristics of a multi-user heating network are related to the length of the heating pipes of each user in the network, and often the length of the heating pipes of each user varies greatly, so it is unrealistic to use a uniform heating temperature at the heat source to ensure that the indoor temperature of all users in a multi-user heating network reaches the same level under the actual situation of changing outdoor temperature. Therefore, it is necessary to install a blocker on the radiator side, which works on the principle of cutting the connection between the radiator and the heating pipe after the indoor temperature reaches a certain level so that the heat at the heat source does not continue to transfer to the user side, and then reconnect the radiator and the heating pipe when the indoor temperature is below a certain value so that the heat at the heat source can be transferred to the user side.

One method of installing blockers is to install a blocker except on the longest user side of the heating pipe (blocker-installation method I). The heating temperature needs to be determined based on the user with the longest pipe length to ensure that all users remain above a minimum room temperature benchmark. Figure 12a shows in this case the trend of the heating temperature, and Figure 12b shows the trend of the indoor temperature under the effect of the heating temperature shown in Figure 12a and this type of blocker installation. Figure 12b shows that the indoor temperature of the three heat consumers' sides is maintained within a certain temperature range suitable for human habitation when using the heating strategy as shown in Figure 12a. However, the changing trend of heating temperature shown in Figure 12a is more complicated and less convenient for the heat source side. The energy consumption of this heating strategy is  $54.1 \text{ W/m}^2$ .

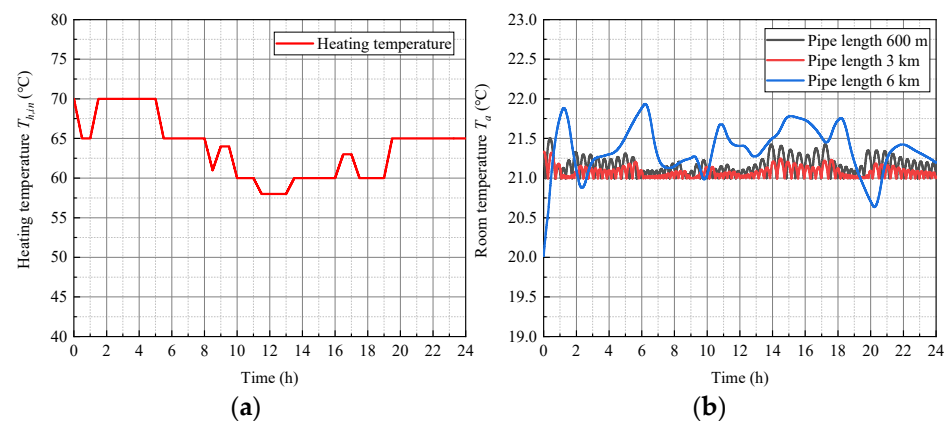


**Figure 12.** (a) Heat supply temperature change and (b) Temperature change of each user under blocker-installation method I.

Another way to install blockers is to install blockers in all users' radiators (blocker-installation method II), and the heating temperature change varies in steps with the outdoor temperature-change trend. The heating temperature and the indoor temperature-variation trend of each user are shown in Figure 13a,b. Figure 13b shows that the room temperature on the user side meets the requirements of human comfort and the variation range of the user with the longest heating pipe is reduced by adopting the heating strategy as shown in Figure 13a. The heating strategy with less change is convenient to operate at the heat source compared with the heating strategy shown in Figure 12a. For the heating strategy shown in Figure 13a, its energy consumption is  $53.8 \text{ W/m}^2$ .

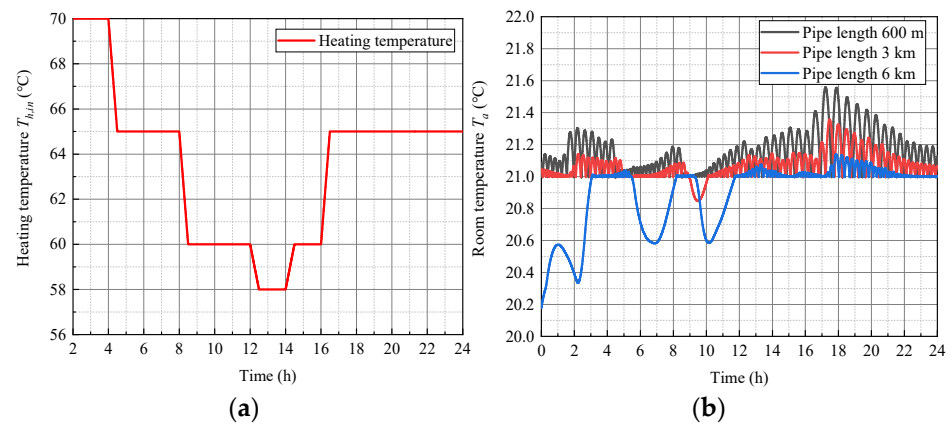


**Figure 13.** (a) Heat supply temperature change and (b) Temperature change of each user under blocker-installation method II.

Comparing the two heating strategies and the blocker-installation methods, it can be concluded that the second method is better than the first one in terms of operational difficulty and energy consumption at the heat source, so the second blocker-installation method will be used as an example in the study of multi-user heating networks facing heating disturbances later in this paper.

#### 4.2. Impact of Heating Fault Disturbance on Multi-User Heating Networks

In daily life, a variety of indoor activities can cause changes in the indoor temperature, such as cooking, using home appliances, partying, etc., thus affecting indoor comfort. In this section, the impact of user-behavior disturbances on multi-user heating networks is studied using dynamic simulation to simulate and consider the impact of heating disturbances. The fault perturbation set is 400 W of heat-source power from 18:00 to 21:00.

The effects caused by the heating disturbance at the same outdoor temperature (Figure 10) and the corresponding heating strategy (Figure 13a) are shown in Figure 14. It is found that with the heat generated by human local activities, the original heating strategy causes large fluctuations in indoor temperature, which affects the user experience. In addition, if the indoor temperature rises too much, it not only affects the user experience but also causes energy waste. Therefore, it is necessary to adopt a new heating strategy to improve the user experience and save energy in the face of heating fault disturbances.

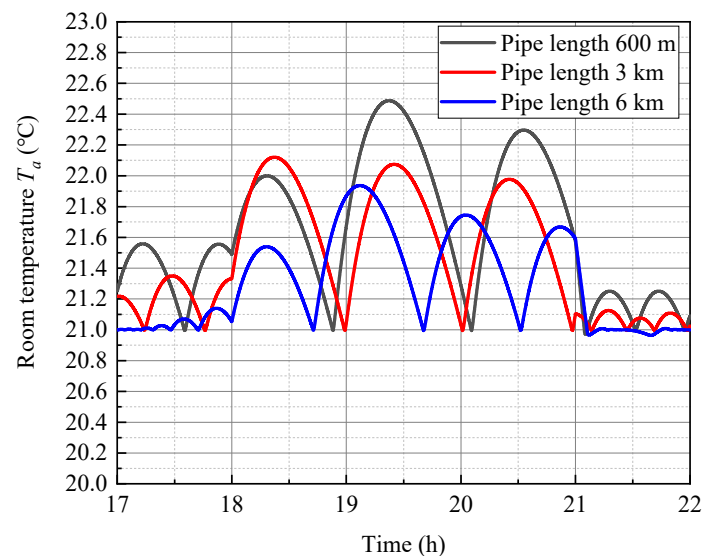


**Figure 14.** Indoor Temperature under Disturbance with Figure 13a Heating Strategy.

#### 4.3. Heating Strategies for Multi-User Heating Networks under Heating Fault Disturbances

Based on the previous subsection, it is evident that a new heating strategy is necessary to cope with the effects caused by heating fault disturbances. This section simulates the use of different heating strategies to cope with the heating disturbances assumed in Section 4.2.

The heating strategy shown in Figure 15a is calculated for the heating fault disturbance. The heating temperature of the new heating strategy adopted in Figure 15a is lower from 17.00 to 20.10 than the heating temperature of the heating strategy adopted in Figure 13a. The energy consumption of the heating network during this time is  $58.2 \text{ W/m}^2$ , and the energy consumption of the heating strategy shown in Figure 13a during the same period is  $67.8 \text{ W/m}^2$ , with an energy saving of about 16.5%. When the multi-user heating network is faced with a heating fault disturbance, the safest time to start the temperature change should be the delayed response time of the user with the shortest heating pipe, but in the case simulated in this paper, from Figure 15b we can see the indoor temperature of the user with the shorter pipe length is higher, so the response strategy adopted is based on the delayed response time of the user with the longest pipe length. The heating-temperature recovery time to the original level should be based on the delayed response time of the user with the longest pipe length. In the simulated case of this paper, the heating temperature recovery time is somewhat later, resulting in a decrease in the indoor temperature of the user with the longest official length as shown in Figure 15b, but it does not affect the heating experience, and thus a more energy-efficient approach is chosen.

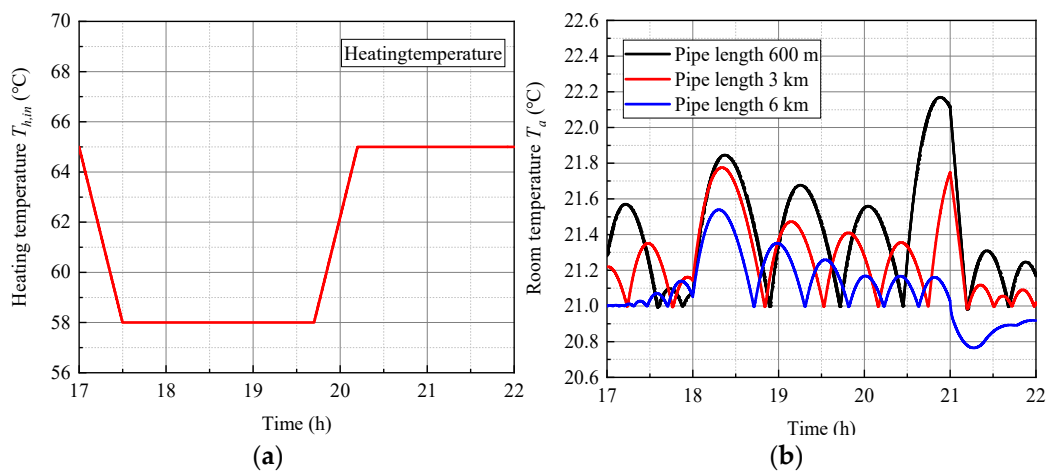


**Figure 15.** (a) Heating strategy for disturbance. (b) Indoor temperature change with new strategy.

## 5. Conclusions

Fault disturbances generated by the behavior of electrical and thermal users in an integrated energy system can greatly affect the system's operational efficiency, and the development of a reasonable anti-fault disturbance strategy is the key to improving the system's operational efficiency. In this paper, for the multi-user heating network in the integrated energy system, the dynamic thermal-power-flow model of each major equipment item in the multi-user heating network and the heating network as a whole is obtained by deriving the RC circuit in the resistance–capacitance reactance principle around heat exchangers, heating pipes and radiators and buildings. Based on the constructed dynamic thermal-power-flow model of the multi-user heating network, the fault-disturbance propagation characteristics are analyzed. The results show that the time required to start the change of indoor temperature of each heat consumer in the multi-user heating network is approximately equal to the delayed response time of the heating pipe, and the longer the pipe length, the smaller the difference between the two times; because there is heat loss during the flow of fluid in the heating pipe, the indoor temperature of heat consumers with different pipe lengths in the multi-user heating network will be different under the action of the same outdoor temperature and heating temperature. The comparison of two anti-

disturbance heating strategies for multi-user heating networks under outdoor temperature disturbance shows that it is easier to operate and more energy-efficient to install blockers on all users' sides when the heating temperature changes with the outdoor temperature step. In order to manage the heating disturbance and outdoor temperature change, the new anti-disturbance heating strategy should be adopted in the multi-user heating network to reduce the large fluctuation of indoor temperature caused by the heating disturbance and reduce the energy consumed by the heating network, and an anti-disturbance smart heating strategy can save about 16.5% of energy.

In this paper, the effect of furniture and appliances, doors, and windows on the heat transfer process in the building is not considered in the modeling of the building, and these factors should be taken into account in the next modeling calculations. The synergistic effect of heat flow regulation and heat temperature regulation should be further investigated in future research.

**Author Contributions:** Investigation, L.S.; Writing—original draft, L.J. and J.P.; Methodology, D.L.; Writing—review and editing, J.P. and L.J.; Conceptualization, K.L. and M.Z. All authors have read and agreed to the published version of the manuscript.

**Funding:** This research was funded by Science and Technology Projects of the State Grid Corporation of China under Project, grant number 5400-202116395A-0-0-00.

**Institutional Review Board Statement:** Not applicable.

**Informed Consent Statement:** Not applicable.

**Data Availability Statement:** Data are contained within the article.

**Conflicts of Interest:** The authors declare no conflict of interest.

## Nomenclature

Character	Physical meaning	Unit
$A$	Area	$m^2$
$C$	Heat capacity	J/K
$G$	Heat capacity flow	W/K
$K$ & $h$	Convection heat transfer coefficient	$W/(m^2 \cdot K)$
$L$	Length	m
$T$	Temperature	K
$\delta$	Thickness	m
$\lambda$	Thermal conductivity	$W/(m \cdot K)$
Subscripts		
$c$	cold-side	
$h$	hot-side	
$in$	inlet	
Abbreviations		
AC	Alternating current	
ACHRA	Acceptance of clean heating in rural areas based on social networks	
BHLP-UN	Base heating load prediction with identifying uncertain thermal disturbance	
DH	District heating	
IMC	Internal model control	
LADRC	Linear Active Disturbance Rejection Control	
PDE	Partial Derivative Equation	
PID	Proportional integral derivative	
RBF	Radial Basis Function	
RC	Resistance capacitance	

## References

1. Hao, J.; Yang, Y.; Xu, C.; Du, X. A Comprehensive Review of Planning, Modeling, Optimization, and Control of Distributed Energy Systems. *Carb Neutrality* **2022**, *1*, 28. [\[CrossRef\]](#)
2. Guo, J.; Wu, D.; Wang, Y.; Wang, L.; Guo, H. Co-Optimization Method Research and Comprehensive Benefits Analysis of Regional Integrated Energy System. *Appl. Energy* **2023**, *340*, 121034. [\[CrossRef\]](#)
3. Luo, X.; Gao, Y.; Liu, X.; Sun, Y.; Li, N.; Liu, J. ACHRA: A Novel Model to Study the Propagation of Clean Heating Acceptance among Rural Residents Based on Social Networks. *Appl. Energy* **2023**, *333*, 120644. [\[CrossRef\]](#)
4. Dai, Y.; Hao, J.; Wang, X.; Chen, L.; Chen, Q.; Du, X. A Comprehensive Model and Its Optimal Dispatch of an Integrated Electrical-Thermal System with Multiple Heat Sources. *Energy* **2022**, *261*, 125205. [\[CrossRef\]](#)
5. Ge, Z.; Fang, W.; Wang, S.; Hao, J.; Yang, Y.; Tian, L.; Sun, J.; Dong, F. Dynamic Modeling and Intelligent Heating Strategies of District Heating System Based on the Standardized Thermal Resistance. *Appl. Therm. Eng.* **2023**, *222*, 119919. [\[CrossRef\]](#)
6. Jiang, M.; Speetjens, M.; Rindt, C.; Smeulders, D. A Data-Based Reduced-Order Model for Dynamic Simulation and Control of District-Heating Networks. *Appl. Energy* **2023**, *340*, 121038. [\[CrossRef\]](#)
7. Zhao, Y.; Ji, X.; Yan, H.; Zhou, S. The Dynamic Properties Modeling of a Heat Exchanger Based on Improved Elman Neural Network. In Proceedings of the 2008 7th World Congress on Intelligent Control and Automation, Chongqing, China, 25–27 June 2008. [\[CrossRef\]](#)
8. Van Dreven, J.; Boeva, V.; Abghari, S.; Grahn, H.; Al Koussa, J.; Motoasca, E. Intelligent Approaches to Fault Detection and Diagnosis in District Heating: Current Trends, Challenges, and Opportunities. *Electronics* **2023**, *12*, 1448. [\[CrossRef\]](#)
9. Huang, P.; Yan, X.; Guo, K. Research and Application of “Internet+” Intelligent Heating System for Central Heating. *Am. J. Eng. Technol. Manag.* **2021**, *6*, 76. [\[CrossRef\]](#)
10. Yang, J.; Peng, M.; Zhao, T.; Cui, M. Modeling and Validation of a Novel Load Model Considering Uncertain Thermal Disturbance in the District Heating System. *Energy Build.* **2023**, *289*, 113055. [\[CrossRef\]](#)
11. Yulong, L. The Stabilisation of a Heat System with Input Delay and Control Matched Disturbance. In Proceedings of the 2019 Chinese Control Conference (CCC), Guangzhou, China, 27–30 July 2019; pp. 1068–1073. [\[CrossRef\]](#)
12. Hua, J.; Yong, C.; Lingdong, L. Application of LADRC Algorithm in Energy-Saving Heating Control System. In Proceedings of the 2021 4th International Conference on Advanced Electronic Materials, Computers and Software Engineering (AEMCSE), Changsha, China, 26–28 March 2021; pp. 120–123.
13. Thenmozhi, M.; Kumar, S.L.; Saranya, S.N. An Evaluation on Optimal Control of Shell and Tube Heat Exchanger for Various Time Delay and Disturbance. In Proceedings of the 2022 6th International Conference on Trends in Electronics and Informatics (ICOEI), Tirunelveli, India, 28–30 April 2022; pp. 56–61.
14. Wei, Z.; Calautit, J. Predictive Control of Low-Temperature Heating System with Passive Thermal Mass Energy Storage and Photovoltaic System: Impact of Occupancy Patterns and Climate Change. *Energy* **2023**, *269*, 126791. [\[CrossRef\]](#)
15. O’Dwyer, E.; De Tommasi, L.; Kouramas, K.; Cychowski, M.; Lightbody, G. Modelling and Disturbance Estimation for Model Predictive Control in Building Heating Systems. *Energy Build.* **2016**, *130*, 532–545. [\[CrossRef\]](#)
16. Kleinertz, B.; Gruber, K. District Heating Supply Transformation—Strategies, Measures, and Status Quo of Network Operators’ Transformation Phase. *Energy* **2022**, *239*, 122059. [\[CrossRef\]](#)
17. Borissova, D.I.; Danev, V.K.; Rashevski, M.B.; Garvanov, I.G.; Yoshinov, R.D.; Garvanova, M.Z. Using IoT for Automated Heating of a Smart Home by Means of OpenHAB Software Platform. *IFAC-Pap.* **2022**, *55*, 90–95. [\[CrossRef\]](#)
18. Lee, Z.E.; Max Zhang, K. Unintended Consequences of Smart Thermostats in the Transition to Electrified Heating. *Appl. Energy* **2022**, *322*, 119384. [\[CrossRef\]](#)
19. Bergsteinsson, H.G.; Nielsen, T.S.; Møller, J.K.; Amer, S.B.; Dominković, D.F.; Madsen, H. Use of Smart Meters as Feedback for District Heating Temperature Control. *Energy Rep.* **2021**, *7*, 213–221. [\[CrossRef\]](#)
20. Jansen, J.; Jorissen, F.; Helsen, L. Optimal Control of a Fourth Generation District Heating Network Using an Integrated Non-Linear Model Predictive Controller. *Appl. Therm. Eng.* **2023**, *223*, 120030. [\[CrossRef\]](#)
21. Chen-xi, J.; Ping, J.; Shi, L. Intelligent Control Method of Heating Process Including Model Prediction and Climate Compensation. In Proceedings of the 2020 International Conference on Advanced Mechatronic Systems (ICAMechS), Hanoi, Vietnam, 10–13 December 2020; pp. 50–55.
22. Kaisermayer, V.; Binder, J.; Muschick, D.; Beck, G.; Rosegger, W.; Horn, M.; Göllles, M.; Kelz, J.; Leusbrock, I. Smart Control of Interconnected District Heating Networks on the Example of “100% Renewable District Heating Leibnitz”. *Smart Energy* **2022**, *6*, 100069. [\[CrossRef\]](#)
23. Desyatirikova, E.N.; Akimov, V.I.; Polukazakov, A.V.; Polyakov, S.I.; Mager, V.E. Development, Modeling and Research of Automation Systems for “Smart” Heating of a Residential Building. In Proceedings of the 2021 IEEE Conference of Russian Young Researchers in Electrical and Electronic Engineering (ElConRus), Moscow, Russia, 26–29 January 2021; pp. 849–854.
24. Zheng, Y.; Feng, S.; Li, N. Optimal Control of Outdoor Transmission and Distribution Pipe Networks for District Heating and Cooling Systems. *Appl. Therm. Eng.* **2023**, *219*, 119592. [\[CrossRef\]](#)
25. Zhang, L.; Du, Y.; Xia, F.; Gao, Y. Two Birds with One Stone: A Novel Thermochromic Cellulose Hydrogel as Electrolyte for Fabricating Electric-/Thermal-Dual-Responsive Smart Windows. *Chem. Eng. J.* **2023**, *455*, 140849. [\[CrossRef\]](#)
26. Lu, N.; Pan, L.; Arabkoohsar, A.; Liu, Z.; Wang, J.; Pedersen, S. Power-Heat Conversion Coordinated Control of Combined-Cycle Gas Turbine with Thermal Energy Storage in District Heating Network. *Appl. Therm. Eng.* **2023**, *220*, 119664. [\[CrossRef\]](#)

27. He, K.-L.; Chen, Q.; Liu, Y.-T.; Hao, J.-H.; Wang, Y.-F.; Yuan, Y. A Transient Heat Current Model for Dynamic Performance Analysis and Optimal Control of Heat Transfer System. *Int. J. Heat Mass Transf.* **2019**, *145*, 118767. [[CrossRef](#)]
28. Hao, J.; Chen, Q.; Li, X.; Zhao, T. A Correction Factor-Based General Thermal Resistance Formula for Heat Exchanger Design and Performance Analysis. *J. Therm. Sci.* **2021**, *30*, 892–901. [[CrossRef](#)]

**Disclaimer/Publisher's Note:** The statements, opinions and data contained in all publications are solely those of the individual author(s) and contributor(s) and not of MDPI and/or the editor(s). MDPI and/or the editor(s) disclaim responsibility for any injury to people or property resulting from any ideas, methods, instructions or products referred to in the content.